

Gap-opening transition and fractal ground-state phase diagram in one-dimensional fermions with long-range interaction: Mott transition as a quantum phase transition of infinite order

Yasuhiro Hatsugai*

Department of Applied Physics, University of Tokyo, 7-3-1 Hongo Bunkyo-ku, Tokyo 113, Japan

(Received 20 January 1997; revised manuscript received 29 May 1997)

The metal-insulator transition in one-dimensional fermionic systems with long-range interaction is investigated. We have focused on an excitation spectrum by the exact diagonalization technique in sectors with different momentum quantum numbers. At rational fillings, we have demonstrated gap opening transitions from the Tomonaga-Luttinger liquid to the Mott insulator associated with a discrete symmetry breaking by changing the interaction strength. Finite interaction range is crucial to have the Mott transition at a rational filling away from the half filling. It is consistent with the strong coupling picture where the Mott gap exists at any rational fillings with sufficiently strong interaction. The critical regions as a quantum phase transition are also investigated numerically. Nonanalytic behavior of the Mott gap is the characteristic in the weak coupling. It is of the order of the interaction in the strong coupling. It implies that the metal-insulator transition of the model is of the infinite order as a quantum phase transition at zero temperature. The fractal nature of the ground-state phase diagram is also revealed. [S0163-1829(97)04143-X]

I. INTRODUCTION

Effects of an electron-electron interaction in electronic systems have become a focus of the condensed-matter physics recently. In a three or higher dimensions, it is widely believed that Landau's fermi-liquid theory is valid and the effect of the interaction is absorbed into several phenomenological Landau parameters. The system is metallic even with the interaction if the ground state is adiabatically connected to the free Fermi sea where the excitations are given by an electron-hole *gapless* excitation across the Fermi surface. In one dimension, however, the ground state is unstable against a perturbation of the interaction and the ground state is given by the so-called Tomonaga-Luttinger (TL) liquid. Although the Fermi-liquid theory is not valid in one dimension, the TL liquid is also metallic and the excitations are gapless. This TL liquid has been focused on again recently and there are a huge number of studies by several techniques such as the bosonization and the conformal field theory.¹⁻⁷ In the paper, we are trying to investigate the breakdown of the TL liquid behavior in a simple fermionic system.^{5,4,12} In a system with periodic potential, that is, on a lattice as a model Hamiltonian, the allowed kinetic energy is restricted by a finite bandwidth. Therefore the strong electron-electron interaction may bring an opening of the energy gap in electronic systems which is known as a Mott transition. The opening of the energy gap implies a metal-insulator transition which has become a focus again in connection to new materials as metal-oxides, organic materials, and the high- T_C superconductors.

As far as the conductivity of the electronic system is concerned, the Mott transition can be understood as a freezing of the charge degree of freedom. There can be spin related phenomena in a small energy scale, however, the Mott transition is a phenomenon of the order of the electron-electron interaction. Noting this fact, we have focused on a charge degree of freedom and chosen a model Hamiltonian of spinless fermions on a lattice,

$$H = -t \sum_j c_{j+1}^\dagger c_j + \text{H.c.} + \sum_{i \neq j} V_{|i-j|} n_i n_j \quad (V_k \geq 0), \tag{1}$$

where the interaction can be long range. (We set $t = 1$ in the following.) When the interaction is nonzero only for the nearest-neighbor (NN) sites, it is mapped to the spin-1/2 antiferromagnetic *XXZ* model by the Jordan-Wigner transformation. In this case, Haldane investigated the model in detail by using the Bethe Ansatz solution of the *XXZ* model.³ Generic ground states of the NN model are the TL liquid without the energy gap except at a half filling where the model has a metal-insulator transition at $V_1 = t$. It is identified as an antiferromagnetic Ising gap in terms of the *XXZ* spin model.

In this paper, we investigate the model, when the interaction is long range, with various filling factors of the fermion numbers. As shown later, it has a rich structure as a *fractal*.

II. STRONG COUPLING

Let us first consider a strong coupling limit $V \gg t$ of the model when the filling factor $\rho = M/L$ is rational, where M is the number of fermions, and L is the number of sites. We use a periodic boundary condition in the following. Let us assume the interaction satisfies the downward convex condition, that is, $(i+j)V_l \leq jV_{l-i} + iV_{l+j}$ ($l < j, l, i, j \leq L$) to avoid a formation of charge clustering. (See later.) A possible form of the interaction which we use in the paper is

$$V_j = V f_j^L(\alpha), \tag{2}$$

$$f_j^L(\alpha) = \frac{1}{\left(\frac{L}{\pi} \sin \frac{j}{L}\right)^\alpha} \quad (\alpha \geq 1), \tag{3}$$

which reduced to a simple power law decaying interaction $V_j = V/j^\alpha$ when $j \ll L$ in a sufficiently large system. The nearest-neighbor interaction can be recovered also by taking

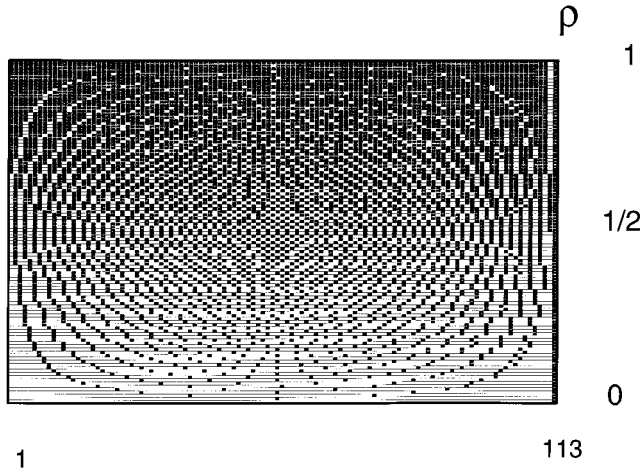


FIG. 1. Ground-state charge ordering of the one-dimensional spinless fermions with long-range interaction in the strong coupling. The black points are the positions of the particles. $\rho = p/q$ with $q = 113$ and $p = 1, \dots, q-1$. The horizontal axis is the spacial direction j , $j = 1, \dots, q-1$.

$\alpha \rightarrow \infty$ and $L \rightarrow \infty$. When the interaction is sufficiently large, the ground state of the system for the rational filling $\rho = p/q$ with mutually prime integers p and q was known for any p and q . It is given by a one-dimensional Wigner crystal with period q .⁸ Although the ground-state charge ordering (crystal structure) is complicated if p and q are large integers, it is explicitly given.⁸ In Fig. 1, the shape of the charge ordering is shown for $\rho = p/q$ with $q = 113$ and $p = 1, \dots, q-1$ as an example. As is expected for the formation of the charge ordering, there are some commensurate conditions to stabilize the system. This commensurability condition brings a fractal structure into the system as shown later. The chemical potential in the thermodynamic limit is evaluated by a similar consideration applied for the long-range Ising model.⁹ It is written as

$$\mu_{\infty}(\rho+0) = V \sum_{k=1}^{\infty} e_{+}(k, \rho) + F(\rho), \quad (4)$$

$$\mu_{\infty}(\rho-0) = V \sum_{k=1}^{\infty} e_{-}(k, \rho) + F(\rho), \quad (5)$$

$$e_{+}(k) = \begin{cases} \left[\frac{k}{\rho} \right] f_{[k/\rho]-1}^{\infty} - \left(\left[\frac{k}{\rho} \right] - 1 \right) f_{[k/\rho]}^{\infty} & \text{if } \left[\frac{k}{\rho} \right] = \frac{k}{\rho} \\ \left(\left[\frac{k}{\rho} \right] + 1 \right) f_{[k/\rho]}^{\infty} - \left[\frac{k}{\rho} \right] f_{[k/\rho]+1}^{\infty} & \text{otherwise,} \end{cases}$$

$$e_{-}(k) = - \left[\frac{k}{\rho} \right] f_{[k/\rho]+1}^{\infty} + \left(\left[\frac{k}{\rho} \right] + 1 \right) f_{[k/\rho]}^{\infty},$$

where $[x]$ is a Gauss symbol which denotes a least integer which is not larger than x and $F(\rho)$ is an order t contribution mainly from the kinetic energy which is a smooth function of ρ . In Fig. 2, the chemical potentials are evaluated for two different interactions. It is a devil's staircase which was first discussed by Bak and Bruinsma in a context of the long-range Ising model.⁹ The discontinuity of the chemical poten-

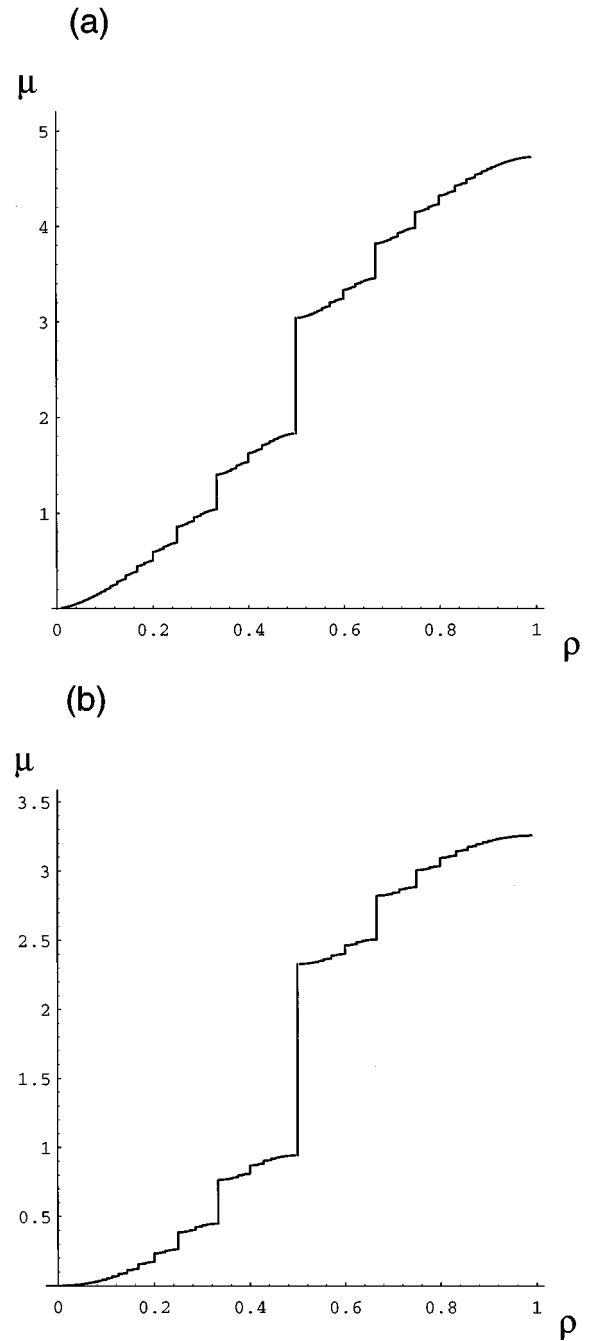


FIG. 2. Evaluation of the chemical potential in the strong coupling limit. The smooth part $F(\rho)$ is set to be zero for simplicity. (a) $\alpha = 2$, (b) $\alpha = 1.5$.

tial, $\Delta\mu$, which is a key quantity to judge whether the system is metallic ($\Delta\mu = 0$) or not ($\Delta\mu > 0$) is evaluated as

$$\Delta\mu_{\infty} \left(\rho = \frac{p}{q} \right) = \mu_{\infty}(\rho+0) - \mu_{\infty}(\rho-0) = Vg(\rho),$$

$$g \left(\rho = \frac{p}{q} \right) = \sum_{s=1}^{\infty} s q (f_{sq+1}^{\infty} + f_{sq-1}^{\infty} - 2f_{sq}^{\infty}). \quad (6)$$

This is generically non-negative for the potential which satisfies the convex downward condition. (If this condition is not satisfied, $\Delta\mu$ can be negative for some filling factor

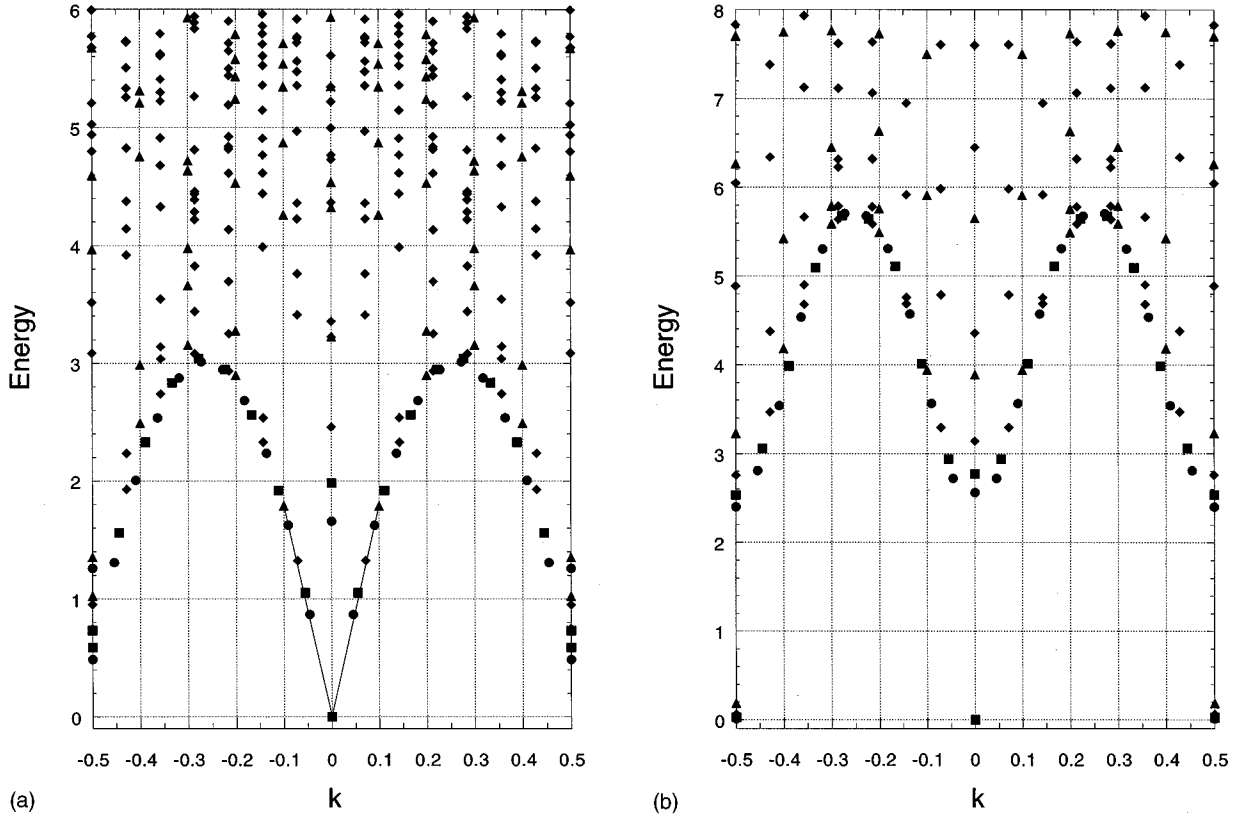


FIG. 3. Low energy spectra of the spinless fermions with long-range interaction classified by the momentum for $\rho=1/2$. ($\alpha=2$). The different symbols are for different system sizes; \triangle : $L=10$, \diamond : $L=14$, \square : $L=18$, \circ : $L=22$. (a) $V=1$. The thin lines are a guide for the eyes. (b) $V=4$.

which causes an instability. It is identified as a charge clustering.) It implies that the energy gap opens for any rational fillings if the interaction is strong enough. Further, as can be seen from Eq. (6), the energy gap $\Delta\mu(p/q)$ only depends on q . Its dependence is given by a power law $\Delta\mu \sim [\rho = (p/q)] \sim (\text{const}/q^\beta)$. From the consideration in the strong coupling limit, to have a Mott insulator phase in the system with filling factor $\rho=p/q$, a finite interaction range over q sites is crucial.

III. WEAK COUPLING

On the other hand, when the interaction is weak ($V \ll t$), the finite bandwidth due to the lattice effect (periodic potential) is not so important. In this case, one can approximate the system as a continuous model with a long range g/r^α interaction and with the periodic boundary condition.¹⁰ When $\alpha=2$, the continuum model is a Sutherland model which has been studied extensively.^{11,13} If $\alpha=2$, the weak coupling model can be discussed using the information from the exact solutions. However, in the strong coupling case, of course, neither of the intermediate coupling cases can be discussed by the exact solutions. The ground state of the Sutherland model is a TL liquid without an energy gap independent of the filling where the ground state is given by the Jastrow wave function.

Noting that there is an energy gap in the strong coupling at a rational filling ρ , it suggests that there is a finite value of the interaction where the energy gap opens. One possibility

is that there is always a nonzero energy gap, that is, the critical value where the energy gap opens, $V_C(\rho)=0$. However, even in the nearest-neighbor model where the energy gap can be most stable, there is a gapless TL phase (XY phase in the XXZ model). Therefore we can expect that there are always finite regions of the gapless TL liquid phases in any filling factors and inevitably the Mott transition.

In the weak coupling, the opening of the energy gap causes an instability of the TL liquid which can be described by the Umklapp operators generated in the higher order in perturbation theory.^{5,4,7} By this perturbational consideration, to have the opening of the energy gap at a higher commensurability, strong repulsion is required. For models with short range interaction (the Hubbard model, etc.), the condition for the instability cannot be satisfied since the so-called TL parameter K can have the restricted value. It implies that the finite range interaction is important to have the instability. This is also consistent with the strong coupling picture.

In the next section, we give numerical results to confirm these considerations (strong coupling and weak coupling) and special efforts are focused on the critical region (intermediate coupling) where the other technique cannot be applied.

IV. NUMERICAL RESULTS AND DISCUSSIONS

As we have discussed, the ground state of the spinless fermions with long-range interaction has two phases for any rational filling when the interaction strength is varied. The

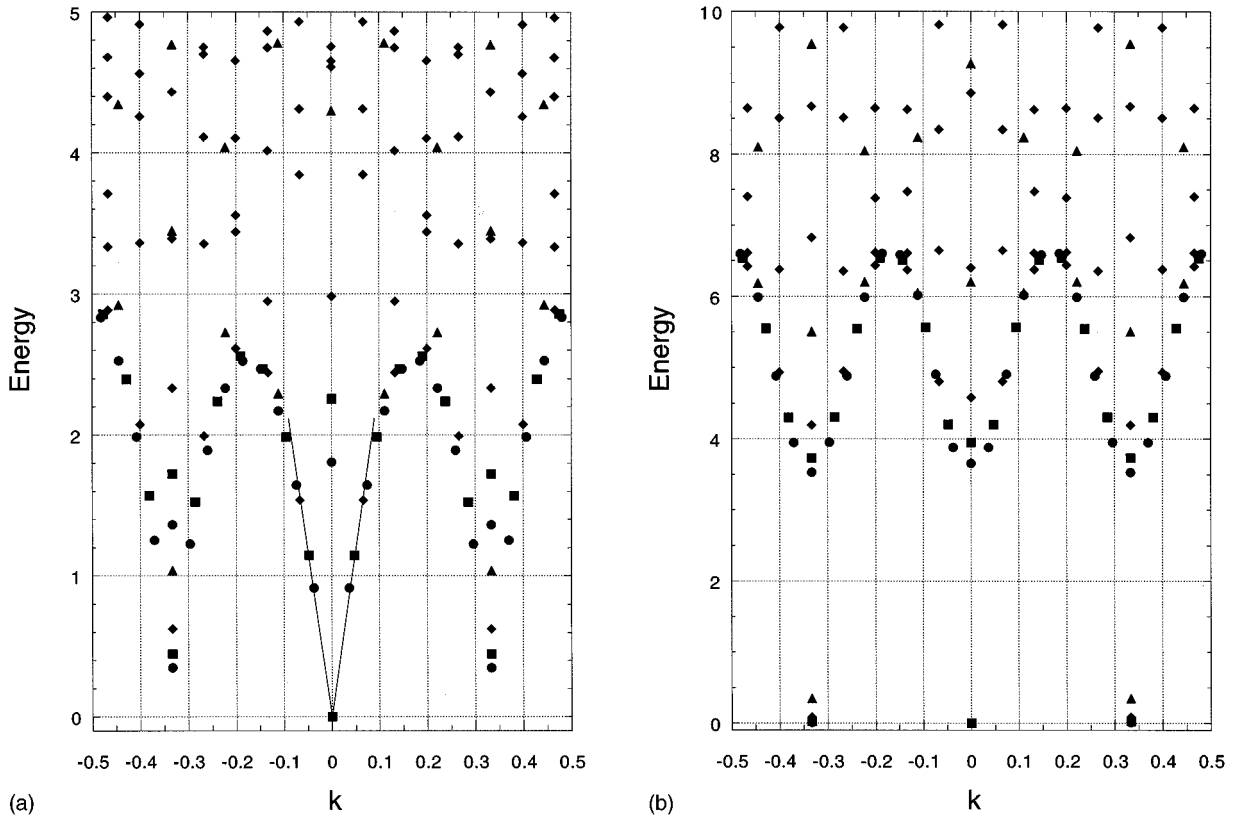


FIG. 4. Low energy spectrum of the spinless fermions with long-range interaction classified by the momentum for $\rho=1/3$. ($\alpha=2$, $t=1$.) The different symbols are for different system sizes; \triangle : $L=9$, \diamond : $L=15$, \square : $L=21$, \circ : $L=27$. (a) $V=4$. The thin lines are a guide for the eyes. (b) $V=32$.

one is the TL liquid metallic phase and the other is the Mott insulator phase. The transition between the two is a typical quantum phase transition at zero temperature. In this section, these phase transitions are demonstrated numerically. The main focus of the numerical calculations here is to investigate a critical behavior near the gap opening (the transition point). Our main strategy is to investigate the system from an insulator side.

We use the exact diagonalization technique for systems with a periodic boundary condition. The Hilbert space is divided into several sectors with different momentum quantum numbers and diagonalized within them to obtain the lowest few energies. For small systems, the full spectra are also obtained. Due to the small system size available, it is not efficient to calculate the chemical potential directly. Instead of it, we calculate an excitation gap E_{ex} which can be comparable with $\Delta\mu$.

In Fig. 3 and Fig. 4, lower parts of energy spectra are shown for systems with $\rho=1/2$ and $\rho=1/3$, respectively. When the interaction is sufficiently weak, one observes a behavior of the gapless TL liquid as shown in Fig. 3(a) and Fig. 4(a). On the other hand, opening of the energy gap near $k=2nk_F$, $n=0, \pm 1, \pm 2, \dots$ ($=2\pi m/q \bmod q$, $m=1, 2, \dots, q$ for $\rho=p/q$) is clearly shown when the interaction is sufficiently strong [see Fig. 3(b) and Fig. 4(b)]. As is known from the strong coupling analysis, there is a discrete symmetry breaking (translational symmetry) in the strong coupling phase. For the $\rho=p/q$ case, this is a Z_q symmetry breaking. Correspondingly there is almost q de-

generate (ground) states in a finite system. They have different total momentum $2nk_F$ ($n=1, \dots, q \bmod q$), respectively. At these momentum sectors, the lowest energy state is given by one of the q degenerate ground states. Therefore the lowest energy gap, the energy difference between the lowest energy state at the momentum and the true ground state of the finite system (usually $k=0$), is related to an energy barrier between the degenerate q ground-states barrier as shown in Eq. (7). The physical energy gap that we are concerned with is the second lowest one as seen in the figures. In the Fig. 5, the lowest energy gap at $k=2k_F$ for $\rho=1/3$ is plotted as a function of the system size for several values of the interaction strength. For $V=32$, the gap size obeys an exponential law as

$$E_{\text{ex}}(k=2k_F, L) \sim e^{-cL}, \quad (7)$$

which is a signature of the (discrete) symmetry breaking and c is the order of the symmetry breaking potential. The discrete symmetry breaking is confirmed numerically for $V=32$ in Fig. 5. To confirm the discrete symmetry breaking, we have also calculated a spectral flow, that is, the energy as a function of the Aharonov-Bohm flux through the periodical system (ring).¹⁴ In Fig. 6, the spectral flows of three different momentum sectors ($k=0$, $2\pi/3$, and $4\pi/3$) for the $\rho=1/3$ system are shown where the Z_3 symmetry breaking is expected. It is clearly shown that the three low energy states are entangled with each other. That is, these three states are equivalent in the thermodynamic limit which is a signature of the discrete symmetry breaking.

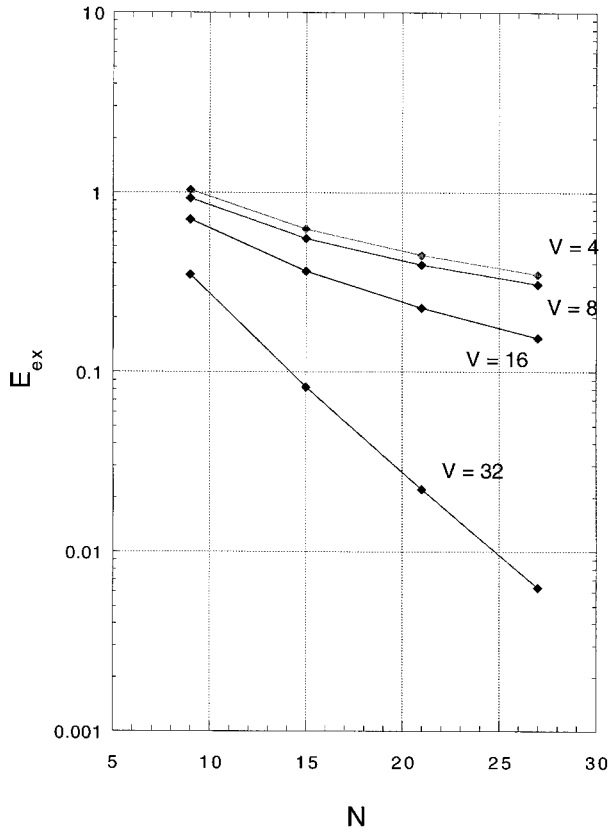


FIG. 5. The energy gap at $k=2k_F$ is shown as a function of the system sizes for $\rho=1/3$ in log scale. ($\alpha=2$). The different lines are for different values of the interaction strength; $V=4, 8, 16$, and 32 from above.

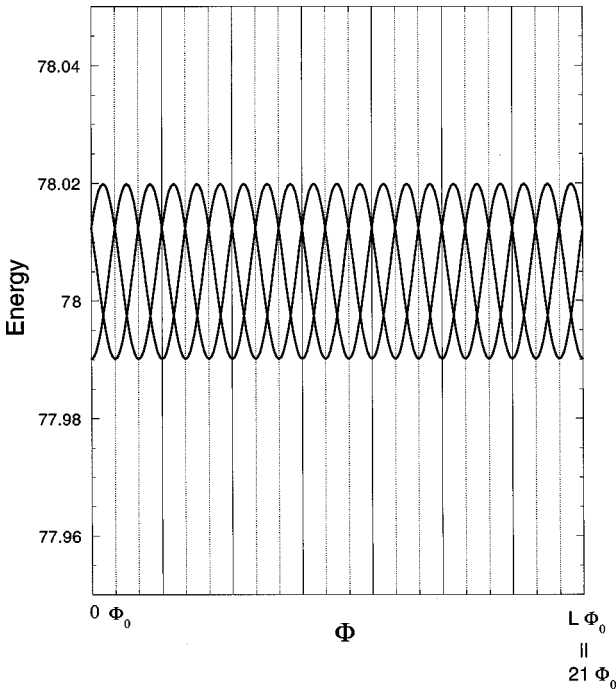


FIG. 6. The spectral flows (energies as a function of the Aharonov-Bohm flux Φ through the ring system) of the three lowest energy states with momentum $k=0, 2\pi/3$, and $4\pi/3$ for the system with the filling factor $\rho=1/3$ ($L=21$). ($\alpha=2$ and $V=32$). Φ_0 is the flux quantum. When $\Phi=L\Phi_0=21\Phi_0$, the system returns to the original state by the (small) gauge invariance.

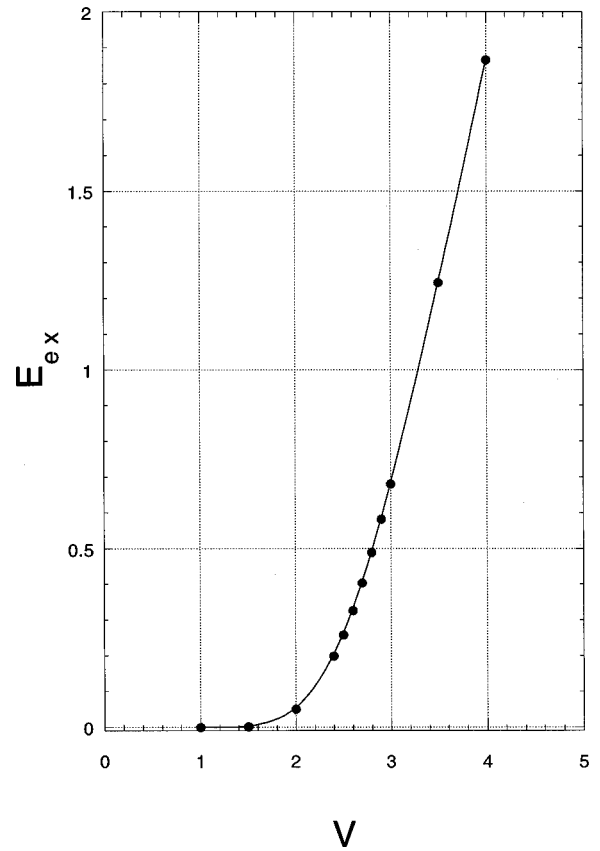


FIG. 7. The excitation gap E_{ex} as a function of V for $\rho=1/2$. ($\alpha=2$). The data are taken by extrapolating to the infinite size.

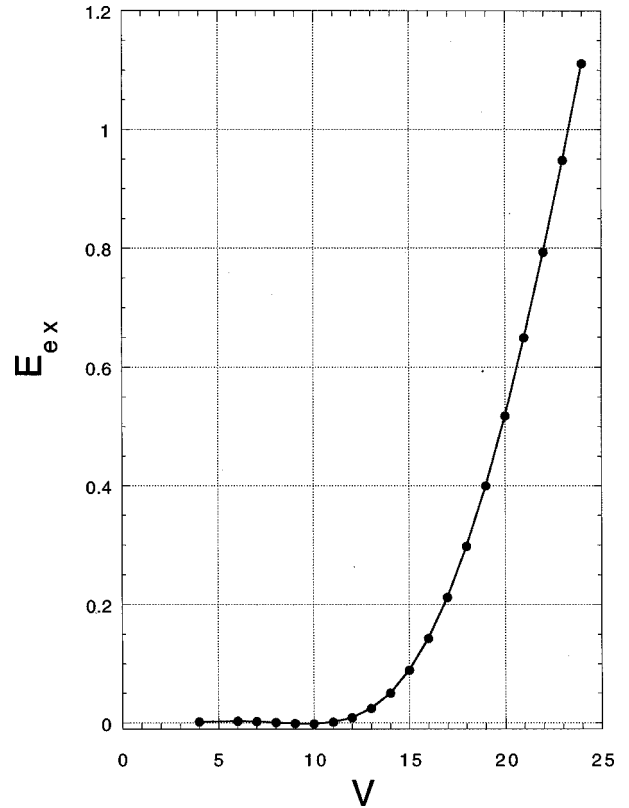


FIG. 8. The excitation gap E_{ex} as a function of V for $\rho=1/3$. ($\alpha=2$). The data are taken by extrapolating to the infinite size.

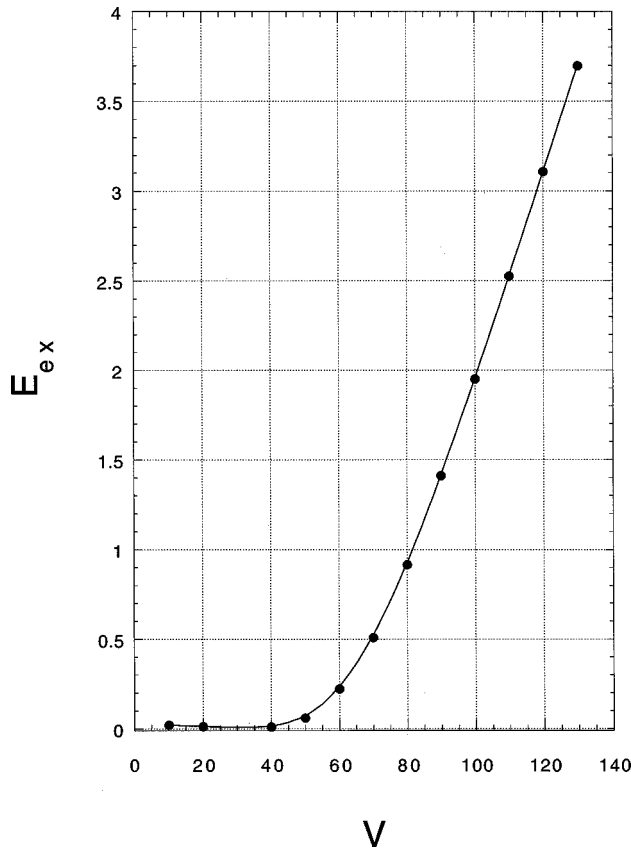


FIG. 9. The excitation gap E_{ex} as a function of V for $\rho=1/4$. ($\alpha=2$). The data are taken by extrapolating to the infinite size limit.

Next let us investigate the critical region. For a nearest-neighbor model at half filling, the behavior of the gap opening is known from the Bethe Ansatz solution and is given by $\Delta\mu \sim \exp(-c/\sqrt{V-V_c})$, which is essentially singular at the critical point.¹⁵ We have numerically investigated the behav-

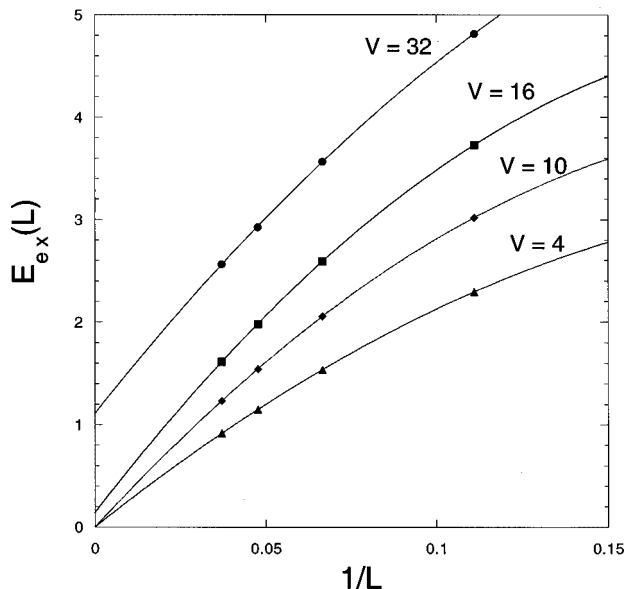


FIG. 10. The excitation gap $E_{\text{ex}}(L)$ as a function of L for several values of V ($\rho=1/3$). ($\alpha=2$). The solid lines are polynomial fits of the data in $1/L$.

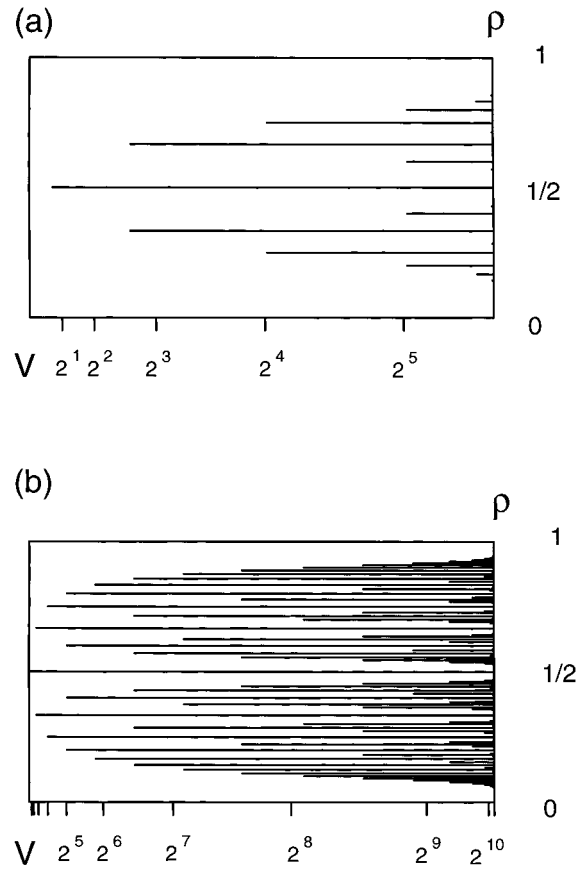


FIG. 11. Estimated ground-state phase diagram of the spinless fermions with long-range interaction. The solid lines are the region with nonzero energy gap. ($\alpha=2$). The rest is a gapless TL liquid. The scale in the horizontal axis is nonlinear as $[(\xi^V-1)/(\xi^V+1)]$; (a) $\xi=1.15$ and (b) $\xi=1.01$. (The strong coupling region is expanded.)

ior of the gap opening for several filling factors in our long-range interaction model. In Figs. 7, 8, and 9, the excitation gap is plotted as a function of the interaction strength.

In the massless TL liquid phase and the Mott insulator phase with Z_q symmetry breaking, $E_0(k=2\pi/L) - E_0(k=0)$ converges to the true energy gap in the thermodynamic limit. Therefore we extrapolate $E_0(k=2\pi/L) - E_0(k=0)$, the energy gap between the lowest energy at $k=0$ and $k=2\pi/L$ to the infinite size limit by fitting them as a polynomial of the $1/L$.

An example of the fitting is shown in Fig. 10 for the $\rho=1/3$ case with several values of the interaction strength. The numerical results shown in Figs. 7, 8, and 9 can be well fitted by the following essentially singular form as a function of the interaction strength,

$$E_{\text{ex}}(V, \rho) \sim c_0(\rho) \exp\left(-\frac{c(\rho)}{[V - V_c(\rho)]^{\gamma(\rho)}}\right) \quad [V \geq V_c(\rho)]. \quad (8)$$

It implies that the transition is a generalized Kosterlitz-Thouless (KT) type. This is also consistent with a fact that the effective Hamiltonian which describes the weak coupling theory is a sine-Gordon Hamiltonian. Here we point out that the possible high symmetry of the transition may cause the *generalized* KT transition. Therefore the transition is of infinite order as a quantum phase transition. This kind of singular behavior is expected in the conformal field theory for the

off-critical behavior near the conformally invariant critical phase. In the $SU(\nu)$ invariant case, the exponent γ is evaluated by the renormalization group analysis to be $\gamma = \nu/(\nu+2)$.¹⁶ At the critical point the model has an apparent Z_q symmetry but may have a higher symmetry. Then one of the possible guesses for the exponent can be $\gamma(\rho = p/q) = q/(q+2)$.

Numerically it is difficult to determine $V_c(\rho)$ and $\gamma(\rho)$ with sufficient accuracies due to the singular behavior of the energy gap. However one may use $V_c(\rho) \sim t/g(\rho)$ as a lower bound of V_c since it is plausible to expect the Wigner crystal at the strong coupling melts near $t \sim \Delta\mu_\infty$. This estimate agrees rather well with numerical results obtained (Figs. 7, 8, and 9). In Fig. 11, we have shown a possible ground-state phase diagram using the above estimate. In the figure, the

interaction strength is plotted in a nonlinear scale. It shows that there is always an insulator phase for any rational filling. Since the $n - \mu_\infty$ curve is the devil's staircase, $\Delta\mu_\infty(\rho)$ shows a fractal structure. Correspondingly, the ground-state phase diagram of the spinless fermions with long-range interaction has a clear *fractal structure*.

ACKNOWLEDGMENTS

The author thanks Y. Morita, M. Kohmoto, M. Takahashi, K. Maki, and D. Lidsky for helpful discussions. This work was supported in part by a Grant-in-Aid from the Ministry of Education, Science and Culture of Japan. The computation in this work has been partly done using the facilities of the Supercomputer Center, ISSP, University of Tokyo.

*Electronic address: hatsugai@coral.t.u-tokyo.ac.jp

¹S. Tomonaga, Prog. Theor. Phys. **5**, 544 (1950).

²V. J. Emery, in *Highly Conducting One-Dimensional Solids*, edited by J. T. Devreese *et al.* (Plenum, New York, 1979); J. Sólyom, Adv. Phys. **28**, 209 (1979), and references therein.

³F. D. M. Haldane, Phys. Rev. Lett. **45**, 1358 (1980).

⁴T. Giamarchi and A. J. Millis, Phys. Rev. B **46**, 9325 (1992); T. Giamarchi, *ibid.* **46**, 342 (1992); Physica B **230-232**, 975 (1997).

⁵H. J. Schulz, in *Strongly Correlated Electronic Materials*, edited by K. S. Bedel (Addison-Wesley, Reading, MA, 1994).

⁶N. Kawakami and S. K. Yang, Phys. Rev. Lett. **65**, 3063 (1990);

Phys. Rev. B **44**, 7844 (1991).

⁷E. B. Kolomeisky, Rev. Mod. Phys. **68**, 175 (1996).

⁸J. Hubbard, Phys. Rev. B **17**, 494 (1978).

⁹P. Bak and R. Bruinsma, Phys. Rev. Lett. **49**, 249 (1982).

¹⁰R. A. Römer and B. Sutherland, Phys. Rev. B **48**, 6058 (1993).

¹¹B. Sutherland, J. Math. Phys. **12**, 251 (1971).

¹²M. Imada, J. Phys. Soc. Jpn. **63**, 3059 (1994).

¹³F. D. M. Haldane, Phys. Rev. Lett. **60**, 635 (1988).

¹⁴K. Kusakabe and H. Aoki, J. Phys. Soc. Jpn. **65**, 2772 (1996).

¹⁵C. N. Yang and C. P. Yang, Phys. Rev. **150**, 321 (1966).

¹⁶C. Itoi and M.-H. Kato, Phys. Rev. B **55**, 8295 (1997).